Neuroscience 284 (2015) 125–133

OPTICAL IMAGING OF THE PROPAGATION PATTERNS OF NEURAL RESPONSES IN THE RAT SENSORY CORTEX: COMPARISON UNDER TWO DIFFERENT ANESTHETIC CONDITIONS

N. HAMA, S.-I. ITO * AND A. HIROTA

Department of Neural and Muscular Physiology, Shimane University School of Medicine, Izumo, Shimane 693-8501, Japan

Abstract—Although many studies have reported the influence of anesthetics on the shape of somatic evoked potential, none has evaluated the influence on the spatio-temporal pattern of neural activity in detail. It is practically impossible to analyze neural activities spatially, using conventional electrophysiological methods. Applying our multiple-site optical recording technique for measuring membrane potential from multiple-sites with a high time resolution, we compared the spatio-temporal pattern of the evoked activity under two different anesthetic conditions induced by urethane or α-chloralose. The somatic cortical response was evoked by electrical stimulation of the hindlimb, and the optical signals were recorded from the rat sensorimotor cortex stained with a voltage-sensitive dye (RH414). The evoked activity emerged in a restricted area and propagated in a concentric manner. The spatio-temporal pattern of the evoked activity was analyzed using isochrone maps. There were significant differences in the latency and propagation velocity of the evoked activity, as well as the full width at half maximum of optical signal between the two anesthetic conditions. Differences in the amplitude and the slope of the rising phase were not significant.

Key words: optical recording, somatosensory cortex, propagation pattern, anesthesia, urethane, α-chloralose.

INTRODUCTION

In the central nervous system, the electrical activities of neurons are closely coupled with one another and exhibit complex spatio-temporal patterns. Conventional electrophysiological methods are insufficient for analyzing these patterns, because of limitations in spatial resolution. The multiple-site optical recording technique using voltage-sensitive dyes (VSDs) has been widely used to the study of spatio-temporal dynamics of sensory responses, in particular in invertebrate ganglia (Salzberg et al., 1977) and in mammalian neocortices (Grinvald and Hildesheim, 2004). A given sensory stimulus induces a propagation of neural excitation wave in the corresponding sensory cortex, e.g. the somatosensory, auditory, visual cortices and so on. This wave, initiated topographically from a small region of the cortex corresponding to the site of the stimulation, propagates to a large cortical area (Orbach et al., 1985; Derdikman et al., 2003; Song et al., 2006; Xu et al., 2007; Han et al., 2008). It is suggested that this propagation of excitatory activity plays an important role in the computation of sensory cortex (Wu et al., 2008; Gao et al., 2012).

Propagation of excitatory responses in the sensory cortex is mediated by the neural circuitry of the neocortex (Tanifuji et al., 1994; Laaris et al., 2000; Song et al., 2006; Wu et al., 2008; Wester and Contreras, 2012). The microcircuitry of the neocortex is constructed by the highly complicated connections of both the excitatory and inhibitory neurons (Douglas et al., 2004). While many studies on the cortical dynamics *in vivo* were so far carried out using anesthetized animals, anesthetization affects the microcircuitry by producing enhancement of inhibition and/or reduction of excitation in cortical neurons. The basic mechanism of anesthesia, i.e., the effects on the synaptic transmission as well as the membrane properties, varies among anesthetic agents (Scholfield, 1980; Garrett and Gan, 1998; Potez and Larkum, 2008). As it generally results in altered behavior of the central nervous system (Winters, 1976; Rojas et al., 2006), the choice of anesthetic is critical for the study of the spatio-temporal dynamics of the evoked activity.

In the present study, we evaluated the influence of anesthetic on the spatio-temporal patterns of stimulus-induced cortical activity using an optical recording system developed in our laboratory (Hirota et al., 1995; Hirota and Ito, 2006; Hama et al., 2010). Two anesthetics, widely used in *in vivo* studies, were examined: urethane and α-chloralose. Anesthetic actions of these agents are long and stable (Rao and Verkman, 2000). However, there are great differences in the effects of these anesthetics on a cellular level (Scholfield, 1980; Garrett and Gan, 1998; Hara and Harris, 2002; Wang et al., 2008). These microscopic differences eventually affect the shape of evoked potentials (Rojas et al., 2006) and, simultaneously, would also affect other macroscopic neural activities such as the propagation of the excitation wave.

*Corresponding author. Tel: +81-853-20-2117; fax: +81-853-20-2115.
E-mail address: ito@med.shimane-u.ac.jp (S.-I. Ito).
Abbreviations: ECoG, electrocorticogram; FWHM, full width at half maximum; VSDs, voltage-sensitive dyes.

http://dx.doi.org/10.1016/j.neuroscience.2014.08.059
0306-4522/

EXPERIMENTAL PROCEDURE

Animals and preparation

Twenty-one female Sprague-Dawley rats weighing 200–300 g, purchased from a commercial supplier (CLEA Japan, Inc., Tokyo, Japan) and maintained with 12-h light–dark cycle before experiment, were anesthetized by intraperitoneal administration of urethane (1.5 g/kg) (n = 10) or α-chloralose (80 mg/kg) combined with urethane (800 mg/kg) (n = 11). These two groups of animals or anesthetic conditions were referred to collectively as 'urethane' and 'α-chloralose' although the latter also contained urethane (cf. Discussion). The depth of anesthesia was monitored using heart rate and electrocorticogram (ECoG) signals and maintained at stage III-3 or 4. Supplemental anesthetic (5% of initial dose) was given via a cannula placed in the femoral vein as necessary. The body temperature of animals was kept at 35 °C with a disposable heating pad. They were then mounted on a stereotaxic instrument and the somatosensory cortex of the left side including hindlimb area was exposed by gentle removal of the skull covering the cortex (semicircle, 10-mm diameter, Fig. 1A). The dura mater overlaying the exposed cortex was left intact. A staining chamber was constructed with dental cement and Vaseline. The surface of the dura mater was cleaned and a solution of VSD (RH414, Molecular Probe, 0.4 mg/ml) in saline (154 mM NaCl, 5.6 mM KCl, 2.2 mM $CaCl_2$), was filled in the chamber for 2 h, with the solution exchanged every 30 min. The stained cortex was then rinsed with fresh saline for 30 min to remove unbound dye. All animal experiments were also performed in compliance with the Guidelines for Animal Experimentation of the Center for Integrated Research in Science, Shimane University.

Optical recording

The detailed method for multiple-site optical recording of neural activity was described in previous papers (Hirota et al., 1995; Hirota and Ito, 2006; Hama et al., 2010). In short, the stained cortex was illuminated with excitation light filtered by band-pass filter (420–590 nm) and the fluorescent light was passed through a long-pass filter (> 640 nm) and detected on a ×6 real image by a 1020-element photodiode array. Since the active element is 1.35 × 1.35 mm in size and separated by insulating area, having width of 0.15 mm, each photodiode received the fluorescence from a 225 × 225-μm region, and pixel interval corresponds to 250 μm on the preparation.

Electrical recording and stimulation

ECoG was recorded with a thin copper wire placed on the surface of the cortex near the edge of recording area. Electrocardiogram was also recorded. To induce a neural response in the somatosensory cortex, an electrical pulse (0.5 ms in duration, 1 mA in intensity) was applied 100 ms after the initiation time of the R wave every 15 or 16 heartbeat, using a pair of tungsten needles inserted under the skin of the hindpaw contralateral to the recording site.

Data analysis

The output from each photo diode was digitized at 1024 Hz and directly stored in a hard disk unit. Reduction of pulsation artifacts was carried out by the procedure described in a previous paper (Hama et al., 2010), and the data of each pixel were filtered using a band-pass filter (0.1–300 Hz) and low-pass filter in space (Gaussian filter, σ = 1, kernel size = 3 × 3 pixels). The

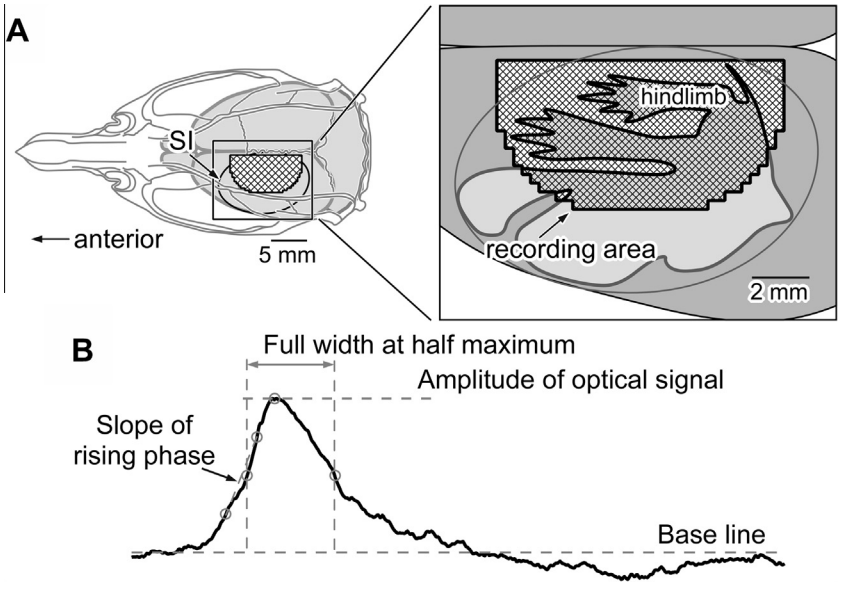

Fig. 1. (A) Location of recording area within the neocortex. Left panel: dorsal view of the recording area with reference to the entire cerebral cortex and the skull. Thick circle indicates the primary somatosensory cortex (SI). The semicircle indicates the recording area. Right panel: magnification of the rectangular area in the left panel. As the somatotopic map shows, the recording area included the hindlimb region. (B) Definition of parameters extracted from the optical signal. See text for details.

fractional change was obtained by dividing the change in fluorescence by the background fluorescence ($\Delta F/F$). The baseline level of optical signal in $\Delta F/F$ was calculated as the average value during 100 ms prior to each stimulation. When the signal during 300 ms after the stimulation exceeded three standard deviations, we defined an evoked response as having been detected. The onset time of the neural response in each pixel was defined as the time for the signal to reach half the peak amplitude. We assumed that only pixels in a five by five matrix contributed to the estimate of the propagation velocity for the pixel of on the center of the matrix. Under this assumption, a two-dimensional Gaussian function for a weighting function can be applied for calculating the weighted mean of time difference normalized by the interval of pixels at the center pixel(x,y), and the equation for the time difference $D(x,y)$ is given by

$$D(x,y)=\frac{\sum_{i=-2}^{2}\sum_{j=-2}^{2}\left(\exp\left(\frac{-(i^2+j^2)}{2}\right)\frac{|\text{latency}(x,y)-\text{latency}(x+i,y+j)|}{\sqrt{i^2+j^2}}\right)}{\sum_{i=-2}^{2}\sum_{j=-2}^{2}\exp\left(\frac{-(i^2+j^2)}{2}\right)}, \quad (1)$$

where x and y are the column- and raw-numbers of pixel; latency(x,y) is the latency at the pixel(x,y). In this equation, each time difference is the absolute value of difference in the latency between a pixel in the matrix and the center pixel. The denominator of the equation is the sum of weights used as multipliers for time difference in the numerator; when the time difference is zero, the corresponding weight value is excluded from summation. If the denominator was below 0.5, that datum was omitted. Using this value, propagation velocity $v(x,y)$ at a pixel(x,y) was calculated as

$$v(x,y)=L/D(x,y), \quad (2)$$

where L is the pixel interval in the array. In this study $L = 250$ μm.

We also analyzed the kinetic parameters of the optical response signals. Three parameters, i.e., the slope of the rising phase, the peak amplitude and the full width at half amplitude, were extracted. The slope of the rising phase was calculated linearly between 25% and 80% of peak amplitude (Fig. 1B). All parameters taken from one animal, including the propagation velocity, were quantified as the mean value of pixels within the annular region around the initiation site (see hatched area in Fig 5A, B). These mean values were further averaged within each group and expressed as mean values ± standard deviation for statistical analyses. We used Welch's t-test for statistical comparisons of data. $p < 0.05$ was considered significant.

RESULTS

Suppressive effect of spontaneous activity on the evoked activity

In this study, spontaneous activities emerged at a high rate and frequently preceded the evoked response by a short interval under both anesthetic conditions (Fig. 2). In these examples, the evoked neural responses were clearly detected after the stimulations indicated by filled triangle while at the stimulations indicated by open triangle spontaneous neural activity preceded the stimulus by a short interval and no evoked response signals were detected. These results are consistent with previous studies, which reported that spontaneous activities of cortical neurons strongly influence the neural activity evoked by sensory stimulation (Arieli et al., 1996; Petersen et al., 2003; Sachdev et al., 2004; Gao et al., 2012).

To visualize the time course of neural activity in the entire recording area under α-chloralose, the amplitude of optical signals in each pixel was coded on a grayscale and displayed every 10 ms (Fig. 3A). In trial 7, the spontaneous activity lasted until 50 ms before stimulation and the evoked neural activity propagated widely. In trial 5, the spontaneous activity was detected even until 40 ms before stimulation and the response activity occurred but did not propagate. These observations suggested that the spontaneous activity occurring during 50 ms before stimulation strongly affected the propagation of the subsequent evoked response. Actually, in trials 1, 2 and 6, after an activity-free interval of more than 50 ms before stimulation, the evoked response occurred and propagated; in contrast, in trials 3, 4 and 5, preceding spontaneous activity did not terminate by 50 ms before stimulation and no evoked response was observed. In the same way, effect of spontaneous activity on the evoked activity was analyzed for urethane anesthesia (Fig. 3B), and it was revealed that spontaneous activities should be terminated by 130 ms before stimulation to obtain an undistorted response activity. On the basis of these observations, we discarded trials in which stimulation was given within 50 ms and 130 ms after spontaneous activity under α-chloralose and under urethane, respectively. To eliminate trial-to-trial variability, we employed averaged data in the following analyses.

Comparison of propagation patterns

Under both anesthetic conditions, the hindlimb stimulation induced a neural response in the entire region of the recording area (Fig. 4A). Latencies of the response differed among pixels (Fig. 4B). The fastest response was observed at the pixel corresponding to the hindlimb region of the somatotopic map, and latencies increased away from this portion, i.e., the evoked response initiated in a small portion and propagated to the entire region of the recording area (Fig. 4C). The latency of the fastest response was significantly shorter under α-chloralose than under urethane (40.4 ± 10.0 ms vs 56.0 ± 10.3 ms, respectively, $p < 0.05$). The duration of depolarization in the position of each pixel was shorter under α-chloralose than under urethane.

To compare the propagating patterns in more detail, we constructed an isochrone map based on the time differences among the onsets of neural response (Fig. 5). Under both conditions, the neural response propagated in a concentric manner during the early stage of propagation (see isochrone curves of 20 ms in Fig. 5A and 70 ms in Fig. 5B). In the late stage (30 ms in Fig. 5A and 80 ms in Fig. 5B), however, the isochrone curves were not circular. The density of

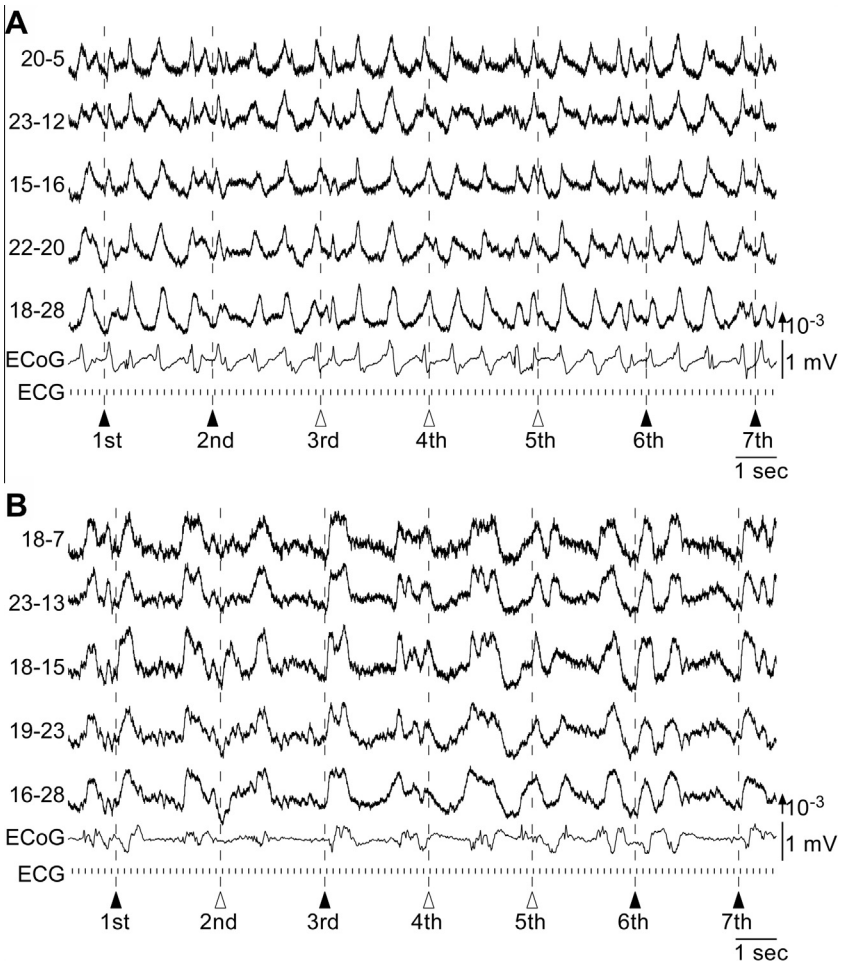

Fig. 2. Trial-to-trial variability of cortical evoked responses. Optical signals recorded from five different sites and the electrocorticogram (ECoG) under different anesthetic conditions (A) α-chloralose, (B) urethane are shown. These traces are of single sweeps after pulsation artifacts were removed. Numerals at the left side of each trace indicate the position of the pixel in the photodiode array (row-column). Dashed lines indicate timings of hindlimb stimulation. ECGs are a raster plot of the initiation time of R-wave detected by the electrocardiogram. In this and following figures, the direction of the arrow in the lower right corner indicates a decrease of fluorescence (corresponding to depolarization), and the length of the arrow represents the stated value of the fractional change (change in fluorescence intensity divided by the resting fluorescence intensity). See text for the meanings of open and filled triangles.

isochrone curves in Fig. 5A was higher than that of Fig. 5B, clearly indicating that the propagation velocity of the response was greater in Fig. 5A than in Fig. 5B. For quantitative comparison, we calculated the velocity. For accurate estimation, we averaged the velocity at pixels in the annular area surrounding the initiation site, e.g. hatched area in Fig. 5A, B, in which the isochrone curves were concentric. The propagation velocity of neural activity was higher under α-chloralose than under urethane (85.6 ± 14.6 μm/ms and 56.2 ± 10.2 μm/ms, respectively, $p < 0.05$, Fig. 5C).

Time course of neural response

The excitation in the whole recording area under α-chloralose ceased by about 250 ms after stimulation. By contrast, under urethane anesthetic the neural activity was still high at the same time point even near the initiation site (Fig. 4C). Thus, the time course of neural response in each recording area apparently differed between the two anesthetic conditions (Fig. 4B) in addition to the propagation velocity. To evaluate the factors contributing to this difference we compared three kinetic parameters of the optical signal; the slope of the rising phase, the peak amplitude and the full width at half maximum (FWHM) (Fig. 6A). The values of these parameters were extracted from the same signals that were used for calculation of the propagation velocity. Neither the slope of the rising phase ($0.21 \times 10^{-4} \pm 0.07 \times 10^{-4}$ ms^{-1} vs $0.17 \times 10^{-4} \pm 0.04 \times 10^{-4}$ ms^{-1}) nor the peak amplitude ($13.5 \times 10^{-4} \pm 2.80 \times 10^{-4}$ vs $14.4 \times 10^{-4} \pm 2.12 \times 10^{-4}$) were different between the two anesthetic conditions (Fig. 6B, C). The difference in FWHM was significant (123 ± 59 ms vs 270 ± 70 ms, $p < 0.05$, Fig. 6D).

DISCUSSION

In the present study, we demonstrated differences in the spatio-temporal pattern of neural activity induced by sensory stimulation under different anesthetic

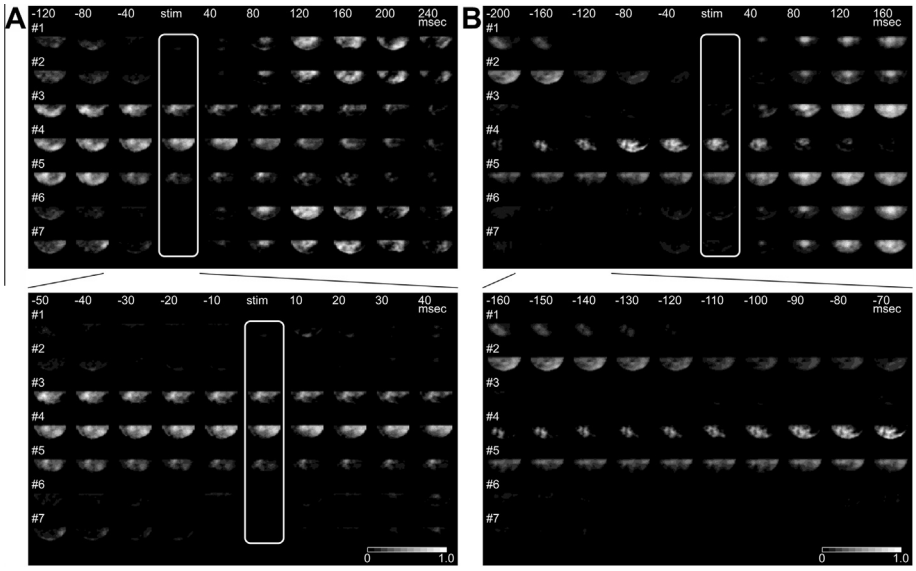

Fig. 3. Effects of spontaneous activity on the spatio-temporal pattern of evoked response under α-chloralose (A) and urethane (B). The amplitude of neural activity at each pixel was normalized to the peak amplitude of the largest response in each trial among whole pixels and coded as a grayscale. The white rectangle corresponds to the time of stimulation. The upper panel is based on about every 40-ms sampling and the lower panel about every 10 ms.

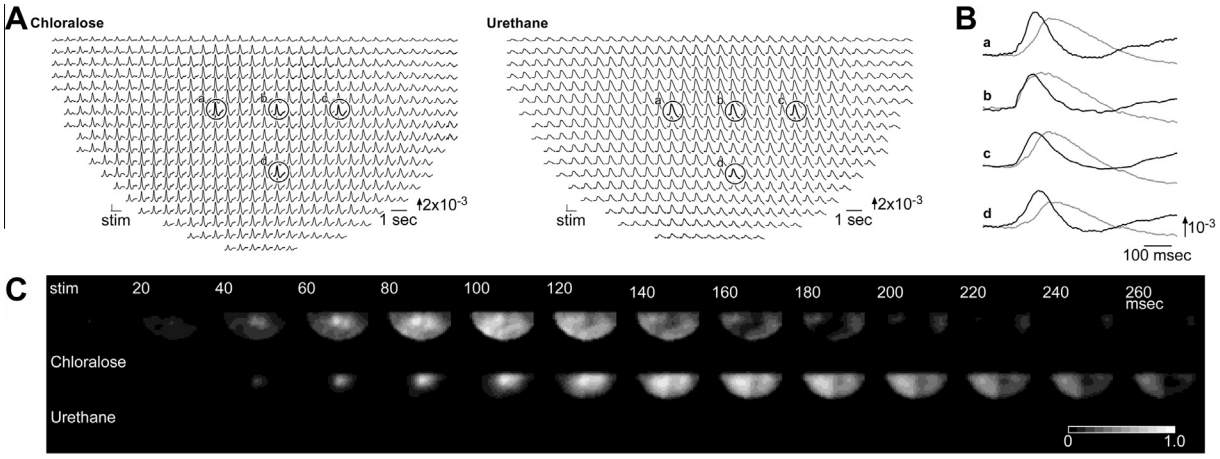

Fig. 4. Evoked responses induced by hindlimb stimulation under different anesthetic conditions. (A) Multiple-site optical recordings of neural response evoked by hindlimb stimulation under different anesthetic conditions (left: α-chloralose, right: urethane). Five traces encircled and labeled a-e are selected and represented in B at an enlarged time scale. The pixel labeled c in each panel indicates the initiation site of neural response. (B) Magnified and superimposed traces obtained from the five sites labeled by a–e in A. Black and gray traces are obtained from chloralose and urethane, respectively. (C) Time-courses of neural activity evoked by hindlimb stimulation under α-chloralose and urethane anesthetics.

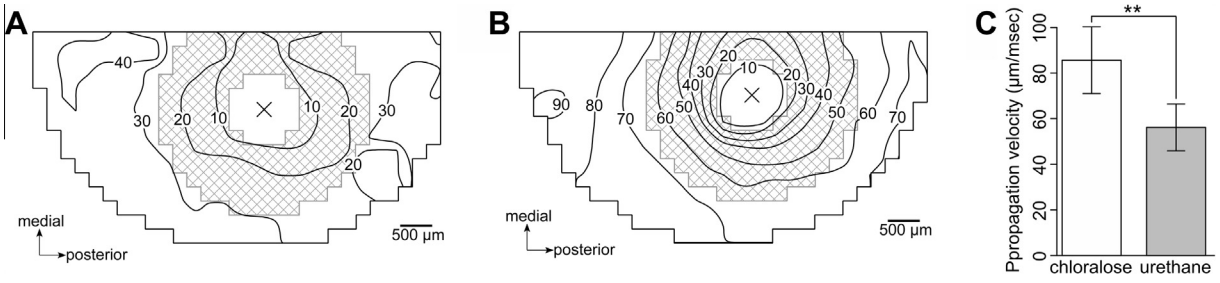

Fig. 5. Comparison of propagation patterns under different anesthetic conditions. (A and B) Isochrone maps of evoked response under α-chloralose (A) and urethane (B) anesthetics. A cross mark in each figure indicates the site where the response first appeared in the observed area. The isochrones represent the delay in the onset time from the cross mark site and the numerals on the curves indicate the delay in milliseconds. The hatched area is the area where the data for following analyses were collected. See text for details. (C) Comparison result of propagation velocities of the evoked responses.

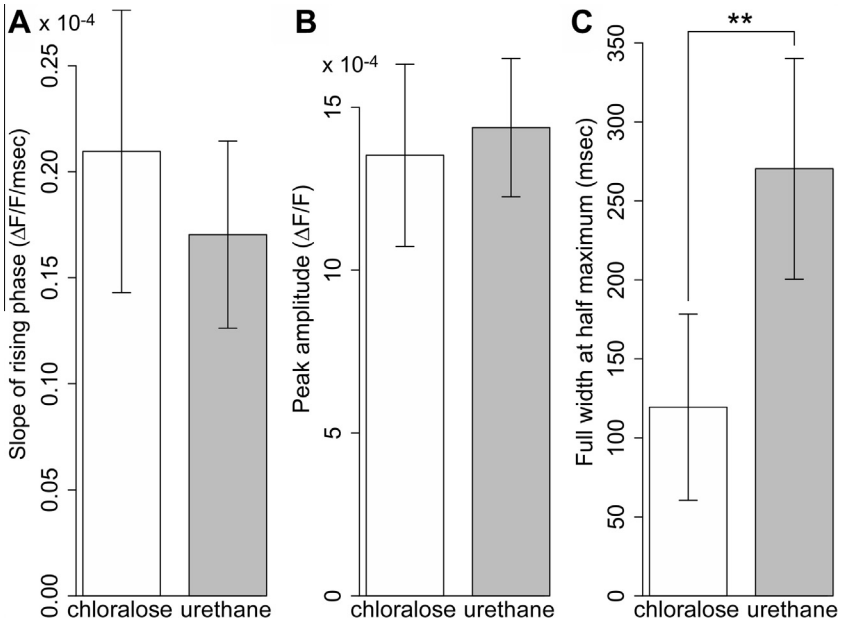

Fig. 6. Comparison of results in the time courses of optical signal. (A–C) Comparison results of slopes of the rising phase, peak amplitudes and full width at half maximum.

conditions. The propagation velocity of neural activity was larger under α-chloralose anesthesia. The duration of the neural excitation was shorter under α-chloralose anesthesia. There was no significant difference in the amplitude of neural response between the two anesthetic conditions.

The evoked response detected by optical methods

The evoked response examined in the present study, even the earliest response detected with optical recording, had much longer latency and duration than those of the typical primary evoked potential in the rat sensorimotor cortex. Nonetheless, this optical signal represented a certain part of the neuronal activity shaping the primary evoked potential; the apparent discrepancy in the time course simply reflects the difference in recording methods, i.e., optical versus electrophysiological. The primary evoked potential consists of two components with different laminar origins: the early surface-positive and the late surface-negative components. The former reflects synaptic activity originating in the middle layer while the latter represents that in the superficial layer (Di et al., 1990). The earliest optical signal in the present study mainly represented the latter activity; two hours of staining was insufficient for the dye RH414 to fully immerse deeper layers, and the signals from these layers, if at all, hardly contributed to the record (unpublished observation). The longer latency of our optical signal is thus attributed to this experimental situation.

Morales-Botello et al. (2012) obtained hind-limb-evoked cortical optical responses with a latency of 23 ms, much shorter than ours and in good agreement with that of the evoked potentials. While their recording procedures were similar to ours, one of the main differences was the choice of VSD; they used RH1691. Petersen et al. (2003) obtained optical signals originating in the layers 2/3 using this same dye, and their vibrissae-related cortical response had a time course comparable to that of the electrophysiological recording from the cell body. The pyramidal cells in layer 3 directly receive the thalamic input (Jensen and Killackey, 1987; Oberlaender et al., 2012). Taken together, it is suggested that throughout the sampled area our optical signals, obtained with dye RH414, originated in layer 2, shallower than those with other dyes or electrophysiological methods.

Propagating velocity

Using optical recording with VSDs, the spreading of neural excitation in a large area of the cortex *in vivo* has frequently been reported (Orbach et al., 1985; Derdikman et al., 2003; Song et al., 2006; Xu et al., 2007; Han et al., 2008). The propagation velocity of the sensory evoked responses was also measured. It differs among sensory cortices; 220 mm/s in the visual cortex, 380 mm/s in the auditory cortex (Song et al., 2006; Wanger et al., 2013) and much smaller values were reported in the somatosensory cortex. Morales-Botello et al. (2012) reported spreading velocities of 80 mm/s and 120 mm/s for the hind-limb and fore-limb responses, respectively. Petersen et al. (2003) reported spreading velocities of 60 mm/s and 33 mm/s in the barrel cortex (in the barrel cortex the velocity differs according to the direction of propagation; the former along the row and the latter along the arc). The values given by these two studies are consistent with our present results (85.6 or 56.2 μm/ms under α-chloralose or urethane, respectively), suggesting that the velocity does not depend on the layers from which propagation signals are recorded.

Anesthetic condition

We used α-chloralose combined with urethane instead of α-chloralose alone. Single use of α-chloralose gives rise

to elevated reflex irritability, causing problems during both surgery and stimulation (Balis and Monroe, 1964; Stamford et al., 1992). Combination with urethane is a common way to avoid this situation, particularly for studies of cortical activity (De Valois and Pease, 1973). This combination, retaining enhanced excitability due to α-chloralose, has been regarded as "α-chloralose anesthesia" in spite of the presence of not a small amount of urethane. In the present study, in addition, spontaneous activity in both ECoG and optical record showed high-amplitude spike-like transients under α-chloralose anesthesia (Fig 2A), which has been recognized as a characteristic accompaniment to α-chloralose anesthesia (Ueki et al., 1988; Peeters et al., 2001; Austin et al., 2005). Meanwhile the differences between the two anesthetic conditions in the present results could also reflect the dose-difference of urethane (0.8 g/kg vs 1.5 g/kg). However, while deep anesthesia reduces the amplitude of the response signal recorded by the optical recording with VSD (Berger et al., 2007; Devonshire et al., 2010), there was no significant difference in the peak amplitudes of response (Fig 6B). Taken together, it appears that the differences of neural response under the two anesthetic conditions observed in this study were largely attributable to the presence of α-chloralose.

Anesthetic agents presumably enhance the inhibition and/or depress the excitation in the central nervous system and reduce the level of consciousness. Although urethane and α-chloralose are both frequently used due to their long-lasting effects, they differ in their actions on neuronal characteristics. Urethane strongly depresses the glutamatergic excitatory transmission (Hara and Harris, 2002), and inhibits the dendritic excitability of cortical pyramidal neurons (Potez and Larkum, 2008). Potentiation of the inhibitory synapse by urethane is minor and its effect varies; at least in the nucleus of the solitary tract it even inhibits the GABAergic transmission (Scholfield, 1980; Hara and Harris, 2002; Sceniak and Maciver, 2006; Accorsi-Mendonça et al., 2007). Urethane enhances an inward current mediated by nicotinic acetylcholine receptor (Hara and Harris, 2002). In the cerebral cortex, nicotine depresses the activity of pyramidal neurons by inhibiting the glutamatergic transmission (Levy et al., 2006) and by exciting some subtypes of GABAergic interneurons (Xiang et al., 1998; Bacci et al., 2005). In contrast, α-chloralose enhances the GABA-induced current by affecting the $GABA_A$ receptor and this effect is stronger than that of urethane (Garrett and Gan, 1998). Its effect on glutamatergic and cholinergic transmission is small or negligible (Wang et al., 2008). Thus, we assume that by altering the strengths of synaptic connections between excitatory neurons and the thresholds of excitatory neurons, anesthetic agents would strongly affect the propagation velocity, as well as the shape, of the excitation wave.

Spatio-temporal pattern in relation to anesthetics

In this study, the anesthetics were administrated systemically, not focally to the cortex. Thus, the anesthetic could have affected any stages of the somatosensory pathway. Indeed, differences in the latency are apparently ascribed to subcortical processes since the onset latency reflects the arrival time of the sensory input at the cortex, and the difference had grown before its arrival. We will not discuss this subject further. On the other hand, the propagation velocity depends on the cortical domain. Propagation waves occur in slice preparations and, moreover, interception of circuits within the cortex interrupts the propagation or decreases the propagation speed (Tanifuji et al., 1994; Song et al., 2006; Wu et al., 2008; Wester and Contreras, 2012). Thus, certain intracortical processes play critical roles in the initiation or sustaining of propagation and are responsible for the velocity. Therefore, our discussion hereafter is focused on the anesthetic effects on cortical neurons.

While the details of neuronal mechanism underlying the propagation of excitation remain unknown, its outline can be traced. The flow of neural activity in the sensory cortex following excitation of thalamic-receiving neurons is divided into vertical and horizontal flows. Interaction of these two flows forms the propagation, with the horizontal flow playing a central role and the vertical one, a modulatory role. Specific thalamic input primarily drives the vertical flow through the intra-columnar neuronal network. The thalamic afferent mainly projects to the spiny cells in layer 4. This input is then relayed to the basal dendrite of the layers 2/3 pyramidal cells, these cells send the output to the layer 5 pyramidal cells which, in turn, make a feedback loop to the layer 2/3 pyramidal cells. Meanwhile, the horizontal flow is mediated by inter-columnar networks, especially those within layer 5 (Tanifuji et al., 1994; Laaris et al., 2000; Sakata and Harris, 2009; Wester and Contreras, 2012). A pyramidal neuron in layer 5 makes excitatory synaptic contacts directly on the basal and the oblique apical dendrites of neighboring pyramidal cells (Markram et al., 1997). The pyramidal neuron also makes feedforward and feedback inhibitions to neighboring pyramidal neurons via GABAergic interneurons (Douglas et al., 2004). These horizontal networks should primarily mediate the propagation of excitation, with each layer 5 neuron activating layer 2/3 neurons within its home column. Of this propagation, the excitatory and inhibitory synaptic activities in layer 5 are undetectable for VSD imaging due to its inability to record from deeper layers. It is the excitation of neurons in layers 2/3, enhanced by neurons in layer 5 (Wester and Contreras, 2012), that VSD imaging detects as the propagation. The velocity of propagation based on VSD imaging thus reflects the process taking place in layer 5, though this is not directly measured.

Factors controlling the velocity of propagation waves were examined. The velocity of epileptiform propagation is reduced by the potentiation of feedforward inhibition (Trevelyan et al., 2007) and the velocity of propagation wave induced by sensory stimulation is reduced by a depression of excitatory synaptic connection (Goulet and Ermentrout, 2011). These findings are consistent with the present results and suggest that the same regulations also apply to the sensorimotor cortex. Since α-chloralose increases the GABAergic transmission and urethane

decreases the glutamatergic transmission, both anesthetic conditions should decrease the propagation velocity, which was just observed in the present study. Although it is premature to estimate, solely based on the previous findings, how and to what extent excitatory or inhibitory synapses influence the net propagation velocity, the present results that the propagation velocity under urethane was significantly slower than that under α-chloralose (Fig. 5) suggest that the influence of the depression of excitatory transmission dominates that of the potentiation of inhibitory transmission on the propagation velocity.

As shown in Fig. 6, the duration of the neural excitation wave was longer under urethane anesthesia. A disynaptic inhibition among pyramidal neurons is induced by high frequency of firing in the neighboring pyramidal neurons (Silberberg and Markram, 2007; Kapfer et al., 2007; Berger et al., 2009). This inhibition would contribute to ceasing processes of the excitation wave. Both the latency and amplitude of this inhibition depend on the firing rate and the number of neighboring pyramidal neurons activated (Silberberg and Markram, 2007; Kapfer et al., 2007). Under urethane anesthesia, the depression of excitatory transmission should block or delay the recruitment of the disynaptic inhibition, inevitably elongating the duration of excitation. Meanwhile, α-chloralose should also block or delay the disynaptic inhibition since GABAergic neurons inhibit the activity of other GABAergic neurons involved in the disynaptic inhibition (Gibson et al., 1999), i.e., potentiation of inhibition in inhibitory-inhibitory wiring causes disinhibition. Thus, both of the anesthetics used can lengthen the duration of the excitation wave. Our results that the duration of the neural excitation wave was longer under urethane anesthesia (Fig. 6D) suggest that alteration of the excitatory synapse has a stronger effect on the duration of excitation than that of the inhibitory synapse.

Perspective

Since the propagation of neural excitation elicited by a sensory stimulation plays an important role in computation by the sensory cortex (Wu et al., 2008; Gao et al., 2012), it is suggested that any alteration of the propagation pattern affects the cortical computation. Therefore, we differentiated the spatio-temporal pattern by alternating anesthetic conditions. Likewise, it is expected that such differentiation also takes place depending on physiological or behavioral conditions. Although modulation of activities in such cases is frequently reported at a single neuron level, there has been less research into whether the propagation pattern is altered at all and, if it actually is, how. As the present study discussed and attributed the alteration to anesthetic-induced differences in excitatory and inhibitory process, it should be possible to be related to the physiology- or behavior-dependent alteration of neuronal activity to cortical microcircuits. Further studies on the spatio-temporal pattern under various conditions that modulate the cortical synaptic process, are required to promote understanding of the mechanism of cortico-computational function.

Acknowledgments—We are grateful to Dr. Kohtaro Kamino for critical reading of the manuscript and constructive comments. This work was partly supported by KAKENHI (20390385, 21650095 and 24700397) from Japan Society for the Promotion of Science.

REFERENCES

Accorsi-Mendonça D, Leão RM, Aguiar JF, Varanda WA, Machado BH (2007) Urethane inhibits the GABAergic neurotransmission in the nucleus of the solitary tract of rat brain stem slices. Am J Physiol Regul Integr Comp Physiol 292:R396–R402.

Arieli A, Sterkin A, Grinvald A, Aertsen A (1996) Dynamics of ongoing activity: explanation of the large variability in evoked cortical responses. Science 273:1868–1871.

Austin VC, Blamire AM, Allers KA, Sharp T, Styles P, Matthews PM, Sibson NR (2005) Confounding effects of anesthesia on functional activation in rodent brain: a study of halothane and α-chloralose anesthesia. Neuroimage 24:92–100.

Bacci A, Huguenard JR, Prince DA (2005) Modulation of neocortical interneurons: extrinsic influences and exercises in self-control. Trends Neurosci 28:602–610.

Balis GU, Monroe RR (1964) The pharmacology of chloralose. A review. Psychopharmacologia 6:1–30.

Berger T, Borgdorff A, Crochet S, Neubauer F, Lefort S, Fauvet B, Ferezou I, Carleton A, Lüscher H, Petersen C (2007) Combined voltage and calcium epifluorescence imaging in vitro and in vivo reveals subthreshold and suprathreshold dynamics of mouse barrel cortex. J Neurophysiol 97:3751–3762.

Berger TK, Perin R, Silberberg G, Markram H (2009) Frequency-dependent disynaptic inhibition in the pyramidal network: a ubiquitous pathway in the developing rat neocortex. J Physiol 587:5411–5425.

Derdikman D, Hildesheim R, Ahissar E, Arieli A, Grinvald A (2003) Imaging spatiotemporal dynamics of surround inhibition in the barrels somatosensory cortex. J Neurosci 23:3100–3105.

De Valois RL, Pease PL (1973) Extracellular unit recording. In: Thompson RF, Patterson MM, editors. Bioelectric recording technique Part A. Cellular processes and brain potentials. New York: Academic Press. p. 95–163.

Devonshire I, Grandy T, Dommett E, Greenfield S (2010) Effects of urethane anaesthesia on sensory processing in the rat barrel cortex revealed by combined optical imaging and electrophysiology. Eur J Neurosci 32:768–797.

Di S, Baumgartner C, Barth DS (1990) Laminar analysis of extracellular field potentials in rat vibrissa/barrel cortex. J Neurophysiol 63:832–840.

Douglas R, Markram H, Martin K (2004) Neocortex. In: Shepherd GM, editor. The synaptic organization of the brain. New York: Oxford University Press. p. 499–558.

Gao X, Xu W, Wang Z, Takagaki K, Li B, Wu J (2012) Interactions between two propagating waves in rat visual cortex. Neuroscience 216:57–69.

Garrett KM, Gan J (1998) Enhancement of gamma-aminobutyric acid A receptor activity by alpha-chloralose. J Pharmacol Exp Ther 285:680–686.

Gibson JR, Beierlein M, Connors BW (1999) Two networks of electrically coupled inhibitory neurons in neocortex. Nature 402:75–79.

Goulet J, Ermentrout GB (2011) The mechanisms for compression and reflection of cortical waves. Biol Cybern 105:253–268.

Grinvald A, Hildesheim R (2004) VSDI: new era in functional imaging of cortical dynamics. Nat Rev Neurosci 5:874–885.

Hama N, Ito S, Hirota A (2010) An improved multiple-site optical membrane potential-recording system to obtain high-quality single sweep signals in intact rat cerebral cortex. J Neurosci Methods 194:73–80.

Han F, Caporale N, Dan Y (2008) Reverberation of recent visual experience in spontaneous cortical waves. Neuron 60:321–327.

Hara K, Harris RA (2002) The anesthetic mechanism of urethane: the effects on neurotransmitter-gated ion channels. Anesth Analg 94:313–318.
Hirota A, Ito S (2006) A long-time, high spatiotemporal resolution optical recording system for membrane potential activity via real-time writing to the hard disk. J Physiol Sci 56:263–266.
Hirota A, Sato K, Momose-Sato Y, Sakai T, Kamino K (1995) A new simultaneous 1020-site optical recording system for monitoring neural activity using voltage-sensitive dyes. J Neurosci Methods 56:187–194.
Jensen KF, Killackey HP (1987) Terminal arbors of axons projecting to the somatosensory cortex of the adult rat. I. The normal morphology of specific thalamocortical afferents. J Neurosci 7:3529–3543.
Kapfer C, Glickfeld LL, Atallah BV, Scanziani M (2007) Supralinear increase of recurrent inhibition during sparse activity in the somatosensory cortex. Nat Neurosci 10:743–753.
Laaris N, Carlson GC, Keller A (2000) Thalamic-evoked synaptic interactions in barrel cortex revealed by optical imaging. J Neurosci 20:1529–1537.
Levy RB, Reyes AD, Aoki C (2006) Nicotinic and muscarinic reduction of unitary excitatory postsynaptic potentials in sensory cortex; dual intracellular recording in vitro. J Neurophysiol 95:2155–2166.
Markram H, Lübke J, Frotscher M, Roth A, Sakmann B (1997) Physiology and anatomy of synaptic connections between thick tufted pyramidal neurones in the developing rat neocortex. J Physiol 500(Pt 2):409–440.
Morales-Botello ML, Aguilar J, Foffani G (2012) Imaging the spatio-temporal dynamics of supragranular activity in the rat somatosensory cortex in response to stimulation of the paws. PLoS One 7:e40174.
Oberlaender M, de Kock CPJ, Bruno RM, Ramirez A, Meyer HS, Dercksen VJ, Helmstaedter M, Sakmann B (2012) Cell type-specific three-dimensional structure of thalamocortical circuits in a column of rat vibrissal cortex. Cereb Cortex 22:2375–2391.
Orbach HS, Cohen LB, Grinvald A (1985) Optical mapping of electrical activity in rat somatosensory and visual cortex. J Neurosci 5:1886–1895.
Peeters RR, Tindemans I, De Schutter E, Van der Linden A (2001) Comparing bold fMRI signal changes in the awake and anesthetized rat during electrical forepaw stimulation. Magn Reson Imaging 19:821–826.
Petersen CCH, Hahn TTG, Mehta M, Grinvald A, Sakmann B (2003) Interaction of sensory responses with spontaneous depolarization in layer 2/3 barrel cortex. Proc Natl Acad Sci U S A 100: 13638–13643.
Potez S, Larkum ME (2008) Effect of common anesthetics on dendritic properties in layer 5 neocortical pyramidal neurons. J Neurophysiol 99:1394–1407.
Rao S, Verkman AS (2000) Analysis of organ physiology in transgenic mice. Am J. Physiol Cell Physiol 279:C1–C18.
Rojas MJ, Navas JA, Rector DM (2006) Evoked response potential markers for anesthetic and behavioral states. Am J Physiol Regul Integr Comp Physiol 291:R189–R196.
Sachdev RNS, Ebner FF, Wilson CJ (2004) Effect of subthreshold up and down states on the whisker-evoked response in somatosensory cortex. J Neurophysiol 92:3511–3521.
Sakata S, Harris KD (2009) Laminar structure of spontaneous and sensory-evoked population activity in auditory cortex. Neuron 64:404–418.
Salzberg BM, Grinvald A, Cohen LB, Davila HV, Ross WN (1977) Optical recording of neuronal activity in an invertebrate central nervous system: simultaneous monitoring of several neurons. J Neurophysiol 40:1281–1291.
Sceniak MP, Maciver MB (2006) Cellular actions of urethane on rat visual cortical neurons in vitro. J Neurophysiol 95:3865–3874.
Scholfield CN (1980) Potentiation of inhibition by general anaesthetics in neurones of the olfactory cortex in vitro. Pflügers Arch 383:249–255.
Silberberg G, Markram H (2007) Disynaptic inhibition between neocortical pyramidal cells mediated by Martinotti cells. Neuron 53:735–746.
Song WJ, Kawaguchi H, Totoki S, Inoue Y, Katura T, Maeda S, Inagaki S, Shirasawa H, Nishimura M (2006) Cortical intrinsic circuits can support activity propagation through an isofrequency strip of the guinea pig primary auditory cortex. Cereb Cortex 16:718–729.
Stamford JA, Crespi F, Marsden CA (1992) In vivo voltammetric methods for monitoring monoamine release and metabolism. In: Stamford JA, editor. Monitoring neuronal activity a practical approach. Oxford: IRL Press. p. 113–145.
Tanifuji M, Sugiyama T, Murase K (1994) Horizontal propagation of excitation in rat visual cortical slices revealed by optical imaging. Science 266:1057–1059.
Trevelyan AJ, Sussillo D, Yuste R (2007) Feedforward inhibition contributes to the control of epileptiform propagation speed. J Neurosci 27:3383–3387.
Ueki M, Linn F, Hossmann K-A (1988) Functional activation of cerebral blood flow and metabolism before and after global ischemia of rat brain. J. Cereb Blood Flow Metab 8:486–494.
Wang K, Zheng C, Wu C, Gao M, Liu Q, Yang K, Ellsworth K, Xu L, Wu J (2008) Alpha-chloralose diminishes gamma oscillations in rat hippocampal slices. Neurosci Lett 441:66–71.
Wanger T, Takagaki K, Lippert MT, Goldschmidt J, Ohl FW (2013) Wave propagation of cortical population activity under urethane anesthesia is state dependent. BMC Neurosci 14:78.
Wester JC, Contreras D (2012) Columnar interactions determine horizontal propagation of recurrent network activity in neocortex. J Neurosci 32:5454–5471.
Winters WD (1976) Effects of drugs on the electrical activity of the brain: anesthetics. Annu Rev Pharmacol Toxicol 16:413–426.
Wu J, Huang X, Zhang C (2008) Propagating waves of activity in the neocortex: what they are, what they do. Neuroscientist 14:487–507.
Xiang Z, Huguenard JR, Prince DA (1998) Cholinergic switching within neocortical inhibitory networks. Science 281:985–988.
Xu W, Huang X, Takagaki K, Wu JY (2007) Compression and reflection of visually evoked cortical waves. Neuron 55:119–129.

(Accepted 26 August 2014)
(Available online 6 October 2014)